Physica D 238 (2009) 1598–1614

Contents lists available at ScienceDirect

Physica D

journal homepage: www.elsevier.com/locate/physd

Bifurcations of mixed-mode oscillations in a stellate cell model

Martin Wechselberger [a,*], Warren Weckesser [b,1]

[a] Department of Mathematics and Statistics, University of Sydney, Australia
[b] Enthought, Inc., 515 Congress Avenue, Suite 2100, Austin, TX 78701, USA

ARTICLE INFO

Article history:
Received 21 August 2008
Received in revised form
20 March 2009
Accepted 27 April 2009
Available online 18 May 2009
Communicated by S. Coombes

PACS:
02.30.Hq
02.30.Oz
87.19.ln

Keywords:
Stellate cell
Canard
Folded node
Mixed-mode oscillation
Relaxation oscillation

ABSTRACT

Experimental recordings of the membrane potential of stellate cells within the entorhinal cortex show a transition from subthreshold oscillations (STOs) via mixed-mode oscillations (MMOs) to relaxation oscillations under increased injection of depolarizing current. Acker et al. introduced a 7D conductance based model which reproduces many features of the oscillatory patterns observed in these experiments. For the first time, we present a comprehensive bifurcation analysis of this model by using the software package AUTO. In particular, we calculate the stable MMO branches within the bifurcation diagram of this model, as well as other MMO patterns which are unstable. We then use geometric singular perturbation theory to demonstrate how the bifurcations are governed by a 3D reduced model introduced by Rotstein et al. We extend their analysis to explain all observed MMO patterns within the bifurcation diagram. A key role in this bifurcation analysis is played by a novel homoclinic bifurcation structure connecting to a saddle equilibrium on the unstable branch of the corresponding critical manifold. This type of homoclinic connection is possible due to canards of folded node (folded saddle-node) type.

1. Introduction

Complex oscillatory patterns known as mixed-mode oscillations (MMOs) [1] have been recorded experimentally from mammalian neurons such as stellate cells within the cortical region [2,3]. Stellate cells are the most abundant cell type in layer II of the medial entorhinal cortex. They control information flow to the hippocampus and they appear to be generators of robust limbic rhythms in the theta frequency range (4–12 Hz). In vitro electrophysiological studies [3] show that, when depolarized, stellate cells develop subthreshold oscillatory (STO) patterns as well as MMO patterns, small amplitude STOs interspersed by large amplitude oscillations. One major challenge is to understand the biophysical mechanism generating STOs and MMOs in single stellate cells.

The observed oscillatory patterns in stellate cells, STOs and MMOs, are an intrinsic cell phenomenon. It has been shown in [3] that these patterns result mainly from the interaction between two currents: a fast persistent sodium current I_{Nap} and a slow hyperpolarization activated current I_h. In [4], they developed a single compartment conductance based model incorporating these currents in addition to standard spiking currents to reproduce many aspects of the stellate cell dynamics. The model is given by a system of seven ordinary differential equations. It consists of the current balance equation

$$C\frac{\mathrm{d}V}{\mathrm{d}t} = I_{\mathrm{app}} - I_{\mathrm{Na}} - I_{\mathrm{K}} - I_\ell - I_h - I_{\mathrm{Nap}} \tag{1}$$

which is defined via Kirchhoff's law where V is the membrane potential (mV), C is the membrane capacitance (μF/cm^2) and I_{app} is an applied external current (μA/cm^2). The sodium current I_{Na} together with the delayed rectifier current I_{K} and the leak current I_ℓ define the standard spiking current, similar to the famous Hodgkin–Huxley equations [5], while the persistent sodium current I_{Nap} and the hyperpolarization activated current I_h are specific for the STOs of stellate cells. All the ionic currents are defined via Ohm's law by

$$\begin{aligned} I_{\mathrm{Na}} &= G_{\mathrm{Na}} m^3 h (V - E_{\mathrm{Na}}) \qquad I_{\mathrm{K}} = G_{\mathrm{K}} n^4 (V - E_{\mathrm{K}}) \\ I_\ell &= G_\ell (V - E_\ell) \qquad I_h = G_h (0.65 r_f + 0.35 r_s)(V - E_h) \\ I_{\mathrm{Nap}} &= G_p p (V - E_{\mathrm{Na}}) \end{aligned} \tag{2}$$

where the parameters G_y and E_y, $y \in \{\mathrm{Na}, \mathrm{K}, l, h, \mathrm{Nap}\}$, are the maximal conductances (mS/cm^2) and reversal potentials (mV)

* Corresponding author. Tel.: +61 293513860.
E-mail addresses: wm@maths.usyd.edu.au (M. Wechselberger), warren.weckesser@gmail.com (W. Weckesser).

[1] W.W. was supported by the University of Sydney Bridging Support Grant.

0167-2789/$ – see front matter © 2009 Elsevier B.V. All rights reserved.
doi:10.1016/j.physd.2009.04.017

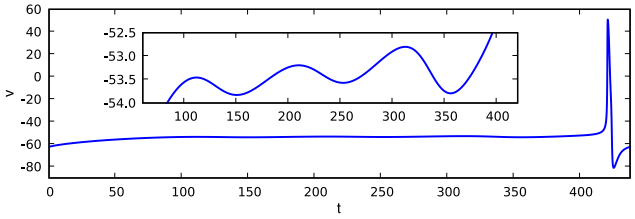

Fig. 1. A stable 1^3 mixed-mode oscillation, $I_{\text{app}} = -2.568$. The inset shows the subthreshold oscillations.

respectively. We use parameter values throughout this paper, as given in [4]. These values can be found in the Appendix.

The conductances of the ionic currents are voltage dependent. This is modelled via dimensionless gating variables (m, h) for I_{Na}, n for I_{K}, (r_f, r_s) for I_h and p for I_{Nap}. Note that the gate h of I_{Na} is the only inactivation gate. All other currents have just activation gates. For $x \in \{m, h, n, p, r_f, r_s\}$, the dynamics of these gates x follow

$$\frac{\mathrm{d}x}{\mathrm{d}t} = \frac{x_\infty(V) - x}{\tau_x(V)} \tag{3}$$

where $x_\infty(V)$, the voltage dependent activation/inactivation curves, and $\tau_x(V)$, the voltage dependent time constants, are given in the Appendix.

Eqs. (1) and (3) define the full seven dimensional model of a stellate cell (7D SC model). Fig. 1 shows one possible MMO pattern obtained with $I_{\text{app}} = -2.568$. In Section 2 we present a comprehensive bifurcation analysis of this model using AUTO [6]. To the best of our knowledge, we calculate, for the first time, MMO branches within such a bifurcation diagram. We further show that these branches terminate in novel homoclinic bifurcation points. This numerical bifurcation analysis is augmented with phase diagrams for better understanding.

In Section 3 we introduce a reduced 3D SC model derived in [7] which describes the dynamics of the full 7D SC model in the subthreshold regime. We are able to confirm with our bifurcation analysis that the 3D SC model indeed covers the dynamics of the 7D SC model, since the corresponding bifurcation diagrams (Figs. 10 and 15) show excellent agreement in the subthreshold regime. Furthermore, this 3D SC model enables us to study the generation of STOs and MMOs with analytical techniques. In particular, [8] identified the canard phenomenon [9–14] to be the mechanism that generates these oscillatory patterns. Here we extend their work and explain the bifurcations of all MMO patterns, stable and unstable, in detail. This is based on defining a global return mechanism for the flow of the 3D SC model that also covers the unstable MMO patterns in the 7D model. We uncover novel homoclinic bifurcation points as part of the canard phenomenon and show how they induce the complicated bifurcation structure. We relate this bifurcation structure in the 3D SC model to canards of folded node and folded saddle-node type. Canards of folded node and folded saddle-node type are also studied in [1,15–20] and have been identified in other neuronal models as well [21–25]. Finally, we conclude in Section 4.

1.1. Numerical methods and computational tools

AUTO [6] was used to compute families of periodic orbits in both stellate cell models (7D and 3D). In the 7D SC model, several families were computed by continuing the periodic orbits that arise at a Hopf bifurcation. Other families were computed by first finding a periodic orbit with some other software and using it as the starting point in AUTO. For most of the families, the starting point was found by using an initial value problem solver to implement a Poincaré map. A stable fixed point of the map was found by simply iterating until the return was sufficiently close to the starting point.

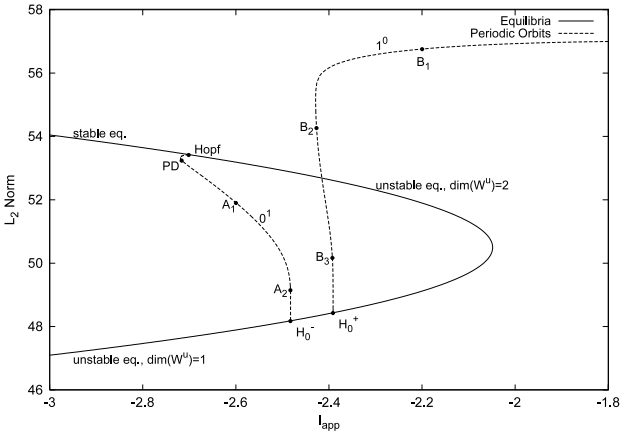

Fig. 2. Bifurcation diagram showing the equilibria and the families of periodic orbits that arise from Hopf bifurcations. The family labeled 1^0 arises from a Hopf bifurcation (near $I_{\text{app}} = 60.7$) that is not shown in this figure. Both families of periodic orbits end as orbits homoclinic to the saddle in the lower branch of equilibria. The homoclinic bifurcation points are labeled H_0^- and H_0^+.

We used the GNU Scientific Library (GSL) ODE solver [26] for the initial value problem solver. In a few cases, the starting point for an AUTO computation was created by altering a numerical solution previously generated by AUTO, either by deleting part of the data or by repeating a part. When computing the periodic orbits in AUTO, mesh sizes ranging from 100 to 800 points were used, with up to five collocation points per mesh interval. The large mesh size was necessary because the problem is singularly perturbed, and because all the families ultimately converged to homoclinic orbits. The computation of a family was halted whenever the period reached 10^7 time units. We consider such a large period to be convincing numerical evidence that the family converges to a homoclinic orbit. Additional maps for the 3D and the 7D SC model were computed with either GSL or MATLAB.

2. Bifurcations in the 7D SC model

The 7D SC model, (1) and (3), was introduced and studied in [4, 7] but no comprehensive bifurcation analysis was undertaken. We are the first to present such a bifurcation analysis with respect to the applied current I_{app}. The bifurcation diagram that we have computed is quite complicated, and is not complete. The system has chaotic invariant sets, so a complete bifurcation diagram of the periodic orbits is not possible. We present various pieces of the bifurcation diagram in stages.

2.1. Equilibria and Hopf bifurcations

We begin with the equilibria. Fig. 2 shows the bifurcation diagram for $-3 < I_{\text{app}} < -1.8$. There is a curve of equilibria, with a subcritical Hopf bifurcation in the upper branch of the curve near $I_{\text{app}} = -2.7$, and a saddle-node bifurcation near $I_{\text{app}} = -2.05$. In the upper branch of equilibria, those to the left of the Hopf bifurcation are stable, and those to the right have a two-dimensional unstable manifold. The equilibria in the lower branch are saddles with one-dimensional unstable manifolds. Also shown in Fig. 2 are two families of periodic orbits. One, labeled 0^1, arises from the subcritical Hopf bifurcation near $I_{\text{app}} = -2.7$, and the other, labeled 1^0, comes from another Hopf bifurcation (near $I_{\text{app}} = 60.7$) that is not shown in the figure.

Fig. 3 shows solutions from the 0^1 family. Near the Hopf bifurcation, these are small orbits, as expected. The solution labeled PD is a period-doubling point. The period-doubled family of solutions that arises from this point will be discussed in Section 2.4.